Damage within a network of white matter regions underlies executive dysfunction in CADASIL

M. O'Sullivan, PhD, MRCP; T.R. Barrick, PhD; R.G. Morris, PhD; C.A. Clark, PhD; and H.S. Markus, DM, FRCP

Abstract—*Objective:* To identify the important sites of white matter disruption that underpin executive dysfunction in CADASIL (cerebral autosomal dominant arteriopathy with subcortical infarcts and leukoencephalopathy), a genetic model of pure subcortical vascular disease. *Methods:* The anatomic pattern of correlation between tissue integrity and executive function was explored with diffusion tensor imaging (DTI), which provides quantitative measures of tissue integrity. Eighteen nondemented patients with CADASIL underwent DTI and cognitive assessment. DTI was normalized to a standard template and correlations assessed at every voxel across the brain with Statistical Parametric Mapping with cluster-level correction for multiple comparisons. *Results:* For executive tasks, correlations were found in a number of discrete regions in the white matter of the frontal lobes. A distinct, nonoverlapping pattern of correlation was seen for verbal memory. Significant independent correlations remained in some regions after co-varying for age and IQ. *Conclusions:* Different cognitive functions correlate with structural integrity at different sites in the white and subcortical gray matter. The distribution of regions correlating specifically with executive function provides clues to the organization of the relevant cognitive networks and their important white matter projections. The cingulum bundle is one candidate tract that may carry anteroposterior connections important for executive processes.

NEUROLOGY 2005;65:1584–1590

Vascular dementia is the second most common cause of dementia worldwide after Alzheimer disease (AD). Up to two-thirds of patients with vascular dementia that are recruited into clinical trials have extensive white matter lesions.[1] In these patients, small vessel cerebrovascular disease, characterized by narrowing of small arteries and arterioles arising on the pial surface of the brain and penetrating to supply the deep white matter, is the predominant pathology. In addition to those with frank dementia, a far larger number of patients with cerebral small vessel disease are likely to have more restricted deficits. The pattern of deficit in these patients is dominated by executive dysfunction.[2,3] Executive function refers to those cognitive abilities by which we marshal and co-ordinate our cognitive resources to respond to complex tasks, optimizing performance when a number of separate cognitive processes are simultaneously at play.[4] Even in the absence of other deficits, executive dysfunction is a major cause of morbidity, dependence, and increased caregiver burden.[5,6] Despite the importance of executive dysfunction in this patient group, the underlying mechanisms of this selective deficit remain obscure. Functional imaging studies have shown that executive tasks often involve a widely distributed network of cortical regions,[7] and one plausible mechanism for executive dysfunction in cerebral small vessel disease is damage to white matter projections, both corticocortical and corticosubcortical, that link these regions into functional networks specific for executive processes.

Diffusion tensor MRI (DTI) is a technique that offers new insights into the role of white matter tracts in cognitive processes. Images are generated that are sensitive to water diffusion within cerebral tissue. In coherent white matter tracts, diffusion is most restricted perpendicular to the direction of the fibers because of the presence of axonal membranes and myelin that act as barriers to diffusion. As these structures degenerate, water diffusivity averaged in all directions (mean diffusivity) increases, and the directionality of diffusion, measured by fractional anisotropy (FA), falls.[8] Previous DTI studies, both in CADASIL (cerebral autosomal dominant arteriopathy with subcortical infarcts and leukoencephalopathy)[9,10] and sporadic small vessel disease,[11] have confirmed that correlations with cognitive function are far more powerful for DTI measures than for lesion volume on T2-weighted images.

Study of the mechanisms of cognitive deficits in sporadic small vessel disease is made difficult by the fact that patients may have other co-existent common pathology. For example, in some series, as many

From Clinical Neuroscience, St George's, University of London, UK.

Disclosure: The authors report no conflicts of interest.

Received April 28, 2005. Accepted in final form August 11, 2005.

Address correspondence and reprint requests to Dr. M. O'Sullivan, Clinical Neuroscience, St George's, University of London, Cranmer Terrace, London SW17 0RE, UK; e-mail: m.osullivan@sghms.ac.uk

as one-third of patients with a diagnosis of vascular dementia are found to have concomitant Alzheimer-type pathology,[12] and risk factors such as hypertension and diabetes mellitus are independently associated with cognitive disturbance. For some diseases, this problem can be avoided by adopting a rare, genetic form of the disease as a pure model of a common disease. This approach has been used successfully in AD[13] and Parkinson disease, where familial forms exist. Similarly, the genetic disease CADASIL is an ideal model for the common sporadic form of diffuse cerebral small vessel disease. A firm diagnosis of CADASIL can be reached by identifying typical pathogenic mutations within the *Notch3* gene.[14] Patients with CADASIL are younger and so are far less likely to have co-morbid AD or other diseases that have an age-dependent incidence. The potential of CADASIL to act as a model has already been exploited to study the role of cholinergic denervation in "pure" vascular dementia.[15] Consistent with this argument, correlations between DTI and executive performance are much stronger for CADASIL than for sporadic small vessel disease. For example, the correlation coefficients between mean diffusivity of normal-appearing white matter and scores on Trail Making and Digit Symbol Tests were 0.67 and −0.62 for CADASIL[16] compared with values of 0.15 and −0.29 in a study of sporadic small vessel disease that adopted identical methodology.[11]

Previous studies therefore support both the potential of CADASIL to act as a model for diffuse white matter disease and the role of DTI as a good technique to explore the consequences of damage to white matter tracts. The purpose of this study was to combine these approaches to improve our understanding of executive dysfunction in white matter disease. Correlations between executive function and white matter damage were examined systematically across the whole brain to determine the sites with the strongest correlations, which are likely to reflect the anatomy of the networks involved in executive function.

Methods. *Subjects.* Eighteen subjects with a diagnosis of CADASIL, confirmed by detection of pathogenic mutations resulting in gain or loss of a cysteine residue in the extracellular portion of the notch 3 protein,[14] were recruited. All were right-handed. No subject met diagnostic criteria for dementia. All had a Mini-Mental State Examination score of 27 or above (mean 29.2 ± 1.0) and were either in the category of cognitive impairment/no dementia (CIND) or had no cognitive symptoms. Mean ± SD age was 46.3 ± 11.1 years. All of the CADASIL subjects underwent conventional MRI, DTI, and neuropsychological assessment.

Cognitive assessment. In all subjects, a cognitive battery was performed, which included a number of tests sensitive to components of executive function: 1) The Trail Making Test was included as a measure of cognitive set shifting and mental flexibility.[17] In part A of the test, the subject is asked to draw a line to join numbered points scattered randomly over a sheet of paper in numerical order. In part B of the test, the test sheet contains points marked by both numbers (1, 2, 3, . . .) and letters (A, B, C, . . .). The subject is asked to join the points with a line, alternating between numerical and alphabetical order (i.e., in the sequence 1, A, 2, B, . . .). Part B therefore differs from Part A in having an executive component but shares similar nonexecutive aspects (visual scanning of the paper and motor function in drawing joining lines). Theoretically, subtracting the time for Part A from that for Part B corrects for differences some of the nonexecutive aspects, so that this B - A score is considered more specific for executive performance. 2) Digit Span Backwards is a measure of working memory performance. Working memory refers to the ability to hold and manipulate information "on-line" for short periods during cognitive processing and is often included under the rubric of executive functioning.[4,18] 3) Digit Symbol is a measure that reflects both performance IQ and executive functioning.[19] Each digit 1 to 9 is ascribed a unique symbol, which the subject is presented in the form of a key. In this test, subjects are presented with a series of digits and are asked to fill in the corresponding symbols in a space below. Subjects are asked to fill in as many consecutive spaces as possible in 90 seconds. This test requires subjects to switch between rules for each digit and therefore requires mental flexibility and has parallels to other set-shifting tasks.

Memory performance was assessed with the Wechsler Memory Scale Paired Associate Learning subtest.[20] Full-scale IQ was estimated with the National Adult Reading Test–Revised.

A composite score (the first principal component) for executive dysfunction, the "executive function score," was generated with principal components analysis. Scores for Digit Span Backwards, Trail Making B-A, and Wechsler Adult Intelligence Scale–Revised Digit Symbol were incorporated into this composite measure.

MRI data acquisition. MRI was performed on a 1.5 T GE Signa MR scanner (Milwaukee, WI). DTI was acquired with a peripherally gated echo-planar imaging sequence with echo time (TE) 121.1 milliseconds, repetition time (TR) 9 R-R intervals on EKG, and maximum strength of diffusion gradients 22 mT/m. In-plane resolution was 1.875 × 1.875 mm. Fifteen to 18 near-axial 5-mm slices with 1-mm gap provided coverage of supratentorial structures in all subjects with a scan time of approximately 4 to 7 minutes. Twenty-eight images were acquired at each slice position with a scheme of diffusion gradient directions optimized for white matter:[21] Twenty-five images acquired with a b factor of 1,000 s/mm^2 and diffusion-encoding gradients evenly distributed in three-dimensional space and three images were acquired without diffusion weighting. An axial fluid-attenuated inversion recovery sequence (TE 135 milliseconds, TR 9,500 milliseconds) was performed and used to calculate total lesion volumes. Multiple contiguous 3-mm slices were prescribed in a true axial plane to provide complete brain coverage. In-plane resolution was 0.86 × 0.86 mm.

Voxel-based correlational analysis. For each slice position, analysis of the DTI data produces mean diffusivity, FA, and T2-weighted images, which are identical in anatomic position. The first step in image processing involved stripping of the skull and dura using an automated algorithm[22] (Brain Extraction Tool; Oxford Centre for Functional Magnetic Resonance Imaging of the Brain; http://www.fmrib.ox.ac.uk/fsl/bet/index.html). For each subject, the T2-weighted images were then fitted to a symmetric echo-planar MRI brain template using a 12-parameter, affine normalization algorithm from Statistical Parametric Mapping[23] (SPM 99, Functional Imaging Laboratory, Institute of Neurology, University College London, UK; http//www.fil.ion.ucl.ac.uk/spm). A symmetric echo-planar template was used. An identical transformation was then applied to the mean diffusivity and FA images. This was repeated for all subjects so that a full set of DT images was produced, all fitted to an identical template. All of the normalized images were reviewed visually to ensure that there were no obvious registration errors. The normalized images were then smoothed using an isotropic Gaussian filter (full width half maximum 4 mm). This process reduces the impact of small errors in registration by recalculating the intensity at each voxel based on a weighted mean of intensity at that voxel and surrounding voxels.

Correlation coefficients were calculated between DTI measurements and each of the cognitive measures at every voxel within the brain across the study group. A significance threshold of $p < 0.001$ was used before correction for multiple comparisons. Correction for multiple comparisons was performed based on the size of a cluster of contiguous "significant" voxels, which is a standard approach in Statistical Parametric Mapping. The basis of this approach is that if voxels are significant by chance, it is most likely that they will be evenly spread throughout the brain. As a cluster increases in size, it becomes less likely that all of the voxels in the

Table 1 *Subject characteristics*

Characteristic	Range	Mean ± SD
Age, y	30–65	46.3 ± 11.1
Neuropsychology		
Premorbid IQ	77–124	107 ± 11
Digit Span Forwards	5–12	7.5 ± 1.9
Digit Span Backwards	3–9	5.7 ± 1.6
WAIS-R Digit Symbol	21–76	45.4 ± 16.9
Trail Making A, s	17–94	41 ± 21
Trail Making B, s	41–189	98 ± 48
FAS Verbal Fluency	4–53	31 ± 14
Paired Associate Learning	4.5–19.0	12.5 ± 4.5
Radiology		
T2 lesion load, cm^3	2.1–139.5	48.4 ± 45.6

WAIS-R = Wechsler Adult Intelligence Scale–Revised.

cluster are "significant" by chance alone.[24] A significance level for the whole cluster of 0.05 was adopted after this correction.

Initially, the composite measure for executive function was correlated with both mean diffusivity and FA. Mean diffusivity correlated most strongly and was therefore chosen to perform subsequent correlation analyses with individual tests. The analyses were repeated with age and premorbid IQ as covariates.

Two procedures were performed to eliminate the effects of CSF contamination. First, all clusters were displayed on a set of T2-weighted images generated from the mean intensities across the whole subject group. Clusters not falling wholly within the brain parenchyma were excluded. Second, scatter plots were generated for all significant clusters, and the clusters were rejected if outlier values due to CSF contamination were identified (mean diffusivity greater than 1.75×10^{-9} m^2/s).

Locations of significant correlations were established by cross-reference with the stereotaxic atlas of Talairach and Tournoux.[25] For peripheral subcortical clusters, not clearly located within a white matter tract depicted in the atlas, their position was recorded with reference to the adjacent cortical region.

Results. The characteristics of the subjects are shown in table 1. None of the subjects had language, attentional, or visual deficits that would have interfered with cognitive testing.

Executive function. Table 2 shows the sites where significant correlations were found between the executive function score and mean diffusivity or FA. In the left cingulum bundle and adjacent to the left precuneus, significant correlations were found with both mean diffusivity and FA. Correlations were stronger and more extensive for mean diffusivity, and a number of additional sites showed correlations between executive function and mean diffusivity only.

To explore these relationships in more detail, correlational analyses were performed for each individual executive test and mean diffusivity. Figure 1 shows the sites where significant correlations were found and tables 3 to 5 provide the SPM99 statistical data. Significant correlations were found only for the "executive" parts of the individual tests. No sites of significant correlation were identified for the nonexecutive control condition (Part A) of the Trail Making Test or for Digit Span Forwards.

There was evidence of anatomic overlap between the regions for different executive tests. A large cluster in the left cingulum bundle was common to Trail Making B-A and Digit Symbol (figure 2), whereas a region of white matter near the left inferior frontal gyrus was a site of significant correlation for both Digit Span Backwards and Trail Making B-A.

Memory. There was no overlap between the regions correlating with verbal memory and those correlating with executive function. For paired associate learning, highly significant clusters were found in the striatum only, bilaterally in the putamina, and in the head of the left caudate nucleus (left putamen T 5.92, $p < 0.001$, right putamen T 5.00, $p = 0.007$, left caudate T 5.07, $p < 0.001$).

Effects of age and premorbid IQ. The correlation analyses were repeated entering both age and premorbid IQ as covariates (see tables 3 to 5). Significant, independent correlations were identified adjacent to the right dorsolateral prefrontal cortex and left inferior frontal white matter for working memory and within the left cingulum bindle for Digit Symbol.

Effect of T2-weighted lesion load. Voxel-by-voxel correlations were also recalculated with lesion volume as a covariate. This did not alter the anatomic pattern of correlations significantly. For Digit Symbol, the correlations in the left cingulum bundle and right cingulum bundle remained highly significant (T 6.87, corrected $p < 0.001$; T 5.67, corrected $p = 0.001$, respectively). For Trail

Table 2 *Composite score for executive function*

Location: white matter structure or adjacent gray matter region (Brodmann area)	Coordinates	Mean diffusivity			Fractional anisotropy		
		T	Size	*p*	*T*	Size	*p*
L medial frontal gyrus (10)	−10, 46, 12	7.18	117	0.001	—	—	—
L precuneus (7)	−8, −50, 50	7.07	125	0.001	5.72	45	0.050
L superior longitudinal fasciculus/superior temporal gyrus (22)	−46, −26, 2	6.75	65	0.028	—	—	—
L cingulum bundle	−18, 2, 28	6.02	220	<0.001	6.02	121	<0.001
L inferior frontal gyrus (9/44)	−38, 0, 32	5.99	111	0.001	—	—	—
L anterior cingulate (32)	−8, 24, 42	5.78	67	0.024	—	—	—
Medial part R superior frontal gyrus (9)	6, 52, 18	5.37	60	0.040	—	—	—
R cingulum bundle	12, −6, 32	5.34	111	0.001	—	—	—
R internal capsule	26, −16, 6	5.28	66	0.026	—	—	—
L centrum semiovale	−36, −38, 22	5.12	122	0.001	—	—	—

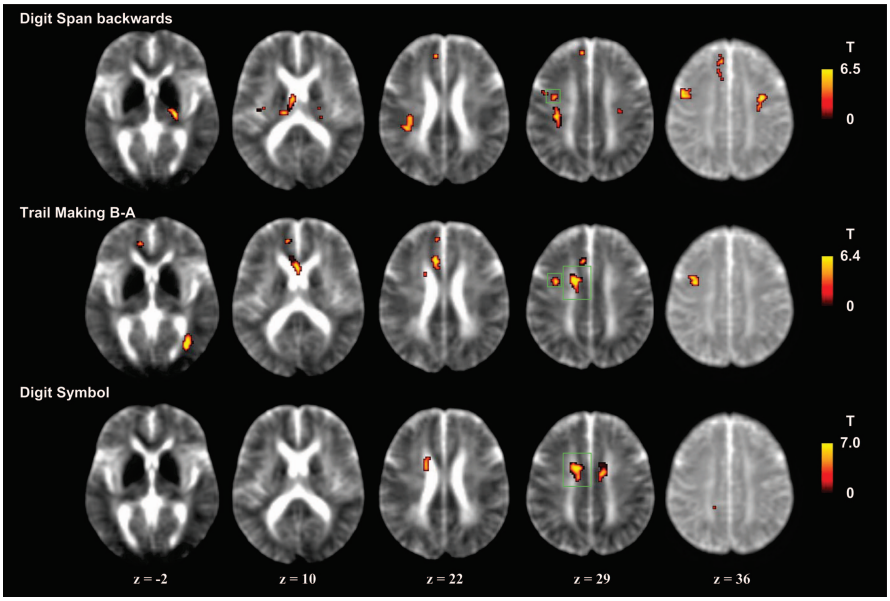

Figure 1. Patterns of correlations between mean diffusivity and executive function. (Top) Digit Span Backwards (a test of working memory). (Middle) Trail Making B-A. (Bottom) Digit Symbol. Regions common to more than one task are highlighted by a green box.

Making B-A, all clusters remained significant except for the left cingulate region, though the left cingulum bundle cluster remained highly significant. Fewer significant clusters were identified for Digit Span Backwards after covarying for lesion volume, but significant clusters were found in identical locations in the left inferior frontal white matter, left superior longitudinal fasciculus, and right inferior longitudinal fasciculus.

Discussion. Executive performance was found to correlate with mean diffusivity in a distributed network of sites in the frontal white matter and the major anteroposterior fasciculus of the cingulum bundle, which connects the frontal lobe with more posterior cortical regions including the hippocampal formation. This pattern of correlation was specific for executive function as a different and distinct pattern of correlation was seen for verbal memory. Although all executive tasks necessarily have some nonexecutive aspects, we found no significant sites of correlation with the nonexecutive control conditions of these tasks. For example, Trail Making A has similar requirements for visual scanning, number sequencing, and motor function as Trail Making B but differs in the need to shift between cognitive sets or rules, and no correlations were found between mean diffusivity and Trail Making A. Similarly, Digit Span Forwards differs from Digit Span Backwards in the demand upon working memory, but no significant sites of correlation were seen for Digit Span Forwards.

As a starting point for this study, the pattern of correlation was assessed with a composite score for executive function that had been found to correlate

Table 3 *Digit Span Backwards*

Location: white matter structure or adjacent gray matter region (Brodmann area)	Coordinates	No covariates			Co-varying for age and IQ		
		T	Size	*p*	*T*	Size	*p*
R internal capsule	24, −22, 0	6.51	93	0.004	—	—	—
L medial frontal gyrus / cingulate (6/8)	−8, 18, 48	6.04	115	0.001	—	—	—
L medial frontal gyrus (8)	−6, 46, 40	5.96	57	0.047	—	—	—
L inferior frontal gyrus (9/44)	−48, 4, 36	5.95	134	<0.001	5.94	61	0.025
R dorsolateral prefrontal cortex (9)	34, −2, 38	5.95	72	0.016	5.88	56	0.037
L superior longitudinal fasciculus/superior temporal gyrus (22)	−38, −42, 18	5.58	177	<0.001	—	—	—
L insula	−40, −16, 18	5.43	61	0.035	—	—	—
R inferior longitudinal fasciculus	50, −14, −14	5.13	63	0.030	—	—	—
L centrum semiovale	−36, −26, 36	—	—	—	6.05	115	0.001
R temporal deep white matter	42, −36, 6	—	—	—	5.22	407	<0.001
L medial frontal gyrus (9)	−10, 42, 26	—	—	—	5.20	103	0.001
L internal capsule	−24, −20, 0	—	—	—	4.85	53	0.048
R medial frontal gyrus (10)	16, 46, 6	—	—	—	4.58	78	0.007

Table 4 *Trail Making B-A*

Location: white matter structure or adjacent gray matter region (Brodmann area)	Coordinates	No covariates			Co-varying for age and IQ		
		T	Size	*p*	*T*	Size	*p*
L medial frontal gyrus (10)	−10, 46, 14	6.38	65	0.037	—	—	—
L cingulate (24/33)	−8, 26, 20	6.20	137	<0.001	—	—	—
L cingulum bundle	−16, 2, 30	5.80	96	0.005	—	—	—
R inferior temporal gyrus (18/19)	36, −70, −2	5.45	125	0.001	5.51	142	<0.001
L inferior frontal gyrus (9/44)	−38, 4, 34	5.34	78	0.015	—	—	—

with DTI in a previous region of interest–based analysis.[16] However, the concept of executive function is broad and encompasses a range of processes, which may have different underlying anatomy, so that the interpretation of such a composite score becomes more difficult at a more detailed anatomic level. The composite score was made up of measures of cognitive set shifting and verbal working memory, and in the analysis of the individual tests, differences in the anatomy of these aspects emerged. No region was found to be common for all three tasks, though a common cluster was shared by both set-shifting tasks.

One robust finding of this study was a correlation for both cognitive set-shifting tasks between performance and mean diffusivity within the left cingulum bundle (see figure 2). This is an intriguing finding as anatomic tracer studies in primates have demonstrated that the cingulum bundle provides a major white matter connection between the dorsolateral prefrontal cortex and more posterior regions.[26] Tracer injections from the middorsolateral prefrontal cortex—but not other prefrontal regions—were carried posteriorly within the cingulum bundle before terminating in the retrosplenial cortex, posterior presubiculum, and the parahippocampal gyrus. In humans, lesions both anteriorly in this system, in the dorsolateral prefrontal cortex, and at its posterior pole in the parahippocampal region can produce deficits of working memory performance.[27] Functional imaging studies of executive tasks also often show activation of posterior regions in addition to areas of the prefrontal cortex.[28,29] Our results suggest that disruption of the connections between the anterior and posterior parts of this network—within the cingulum bundle—may be a mechanism of executive dysfunction in white matter disease.

Verbal working memory tasks preferentially activate the left hemisphere,[30,31] and this asymmetry in cortical activation was reflected at the white matter level in the current study, with clear asymmetry and more significant clusters in the left hemispheric white matter for Digit Span Backwards.[32] Studies of the verbal component of working memory, and more specifically the "articulatory loop" that forms part of the working memory apparatus, have revealed activations in left hemisphere regions associated with language such as the supramarginal gyrus and Broca area.[33] The site of correlation identified in the white matter adjacent to the left inferior frontal gyrus (Brodmann area 44) could represent white matter connections between Broca area and other components of the "articulatory loop."

The distribution of correlations was not altered by co-varying for total lesion volume on T2-weighted images, suggesting that this anatomic pattern reflects the importance of the underlying white matter structures, not the distribution of visible lesions. Indeed, DTI changes both within[9] and outside visible T2-weighted lesions[16] have been shown to correlate with cognitive measures, which is consistent with this interpretation. Many of the correlations were no longer significant when age and premorbid IQ were added as covariates, though significant independent correlations were still observed in the left cingulum bundle for Digit Symbol and left inferior frontal and right dorsolateral prefrontal regions for working memory. Age is a potential confounder because age-related cognitive changes have been shown to correlate with DTI. However, simply using age as a covariate is likely to be excessively stringent as this also removes the effect of disease progression in CADASIL with increasing age. The appearance of additional significant clusters present only in the covaried models for working memory is likely to reflect the fact that performance on this test was particu-

Table 5 *Digit Symbol*

Location: white matter structure or adjacent gray matter region (Brodmann area)	Coordinates	No covariates			Co-varying for age and IQ		
		T	Size	*p*	*T*	Size	*p*
L cingulum bundle	−18, 2, 28	6.95	164	<0.001	5.74	58	0.044
L precuneus (7)	−8, −50, 48	5.81	64	0.034	—	—	—
R cingulum bundle	14, −2, 30	4.95	85	0.008	—	—	—

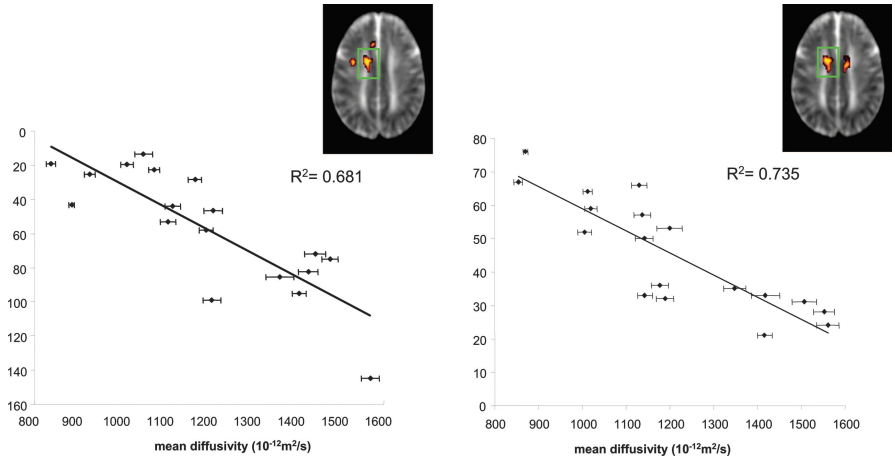

Figure 2. Cognitive set-shifting and the left cingulum bundle. On the scatter plots, each point represents an individual subject and plots mean diffusivity, averaged for the whole significant cluster, against performance. Insets show the clusters for each task. (Left) Trail Making B-A (s). (Right) Digit Symbol. Note that the values on the y axis have been reversed for Trail Making B-A to emphasize that performance declines as mean diffusivity in the cluster increases for both tasks (reflected as an increase in the time to complete Trail Making and a reduction in the number of correct responses for Digit Symbol).

larly susceptible to influence by premorbid intelligence so that removing this source of variance would have strengthened correlations with DTI measures.

Although we were able to demonstrate correlations within some major white matter structures like the internal capsule, cingulum bundle, and superior and inferior longitudinal fasciculi, in many cases, the exact white matter fibers involved and their origins and destinations were obscure. Diffusion tensor MRI is the first technique to reveal the architecture of white matter in vivo, and interpretation is hampered by the fact that the level of detail offered by DTI is not matched by existing anatomic atlases, which include little detail about white matter structure. Advances in the analysis of DT images such as the development of fiber-tracking techniques[34,35] should allow better identification of the connections involved and allow us to interpret correlations at particular sites within the context of reconstructions of important fiber pathways. Improvements in the spatial resolution of DTI and in the co-registration of DT images should also help to localize important connections more precisely. Current technical limitations are also likely to account for the lack of correlation with FA for many of the sites. FA varies much more voxel to voxel than does mean diffusivity, so small errors in image registration are likely to have a greater effect in attenuating any correlations. FA is thought to be particularly well suited to assessing change within coherent white matter tracts, so with development of the techniques, this measure may well provide important additional information.

This study supplements previous DTI studies in CADASIL by adding a new level of anatomic detail to the relationship between white matter damage and cognitive dysfunction. The observation of a network of white matter regions that correlated specifically with executive performance is likely to provide clues to the neural circuitry involved in these processes. The insights provided by DTI will complement those from functional imaging. Although CADASIL is relatively rare, it provides an attractive disease model that should help us to improve our understanding of the mechanisms of cognitive impairment in common diseases such as subcortical vascular disease.

References

1. Erkinjuntti T, Kurz A, Gauthier S, Bullock R, Lillenfield S, Damaraju CV. Efficacy of galantamine in probable vascular dementia and Alzheimer's disease combined with cerebrovascular disease: a randomised trial. Lancet 2002;359:1283–1290.
2. Gupta SR, Naheedy MH, Young JC, Ghobrial M, Rubino FA, Hindo W. Periventricular white matter changes and dementia: clinical, neuropsychological, radiological, and pathological correlation. Arch Neurol 1988; 45:637–641.
3. Junque C, Pujol J, Vendrell P, et al. Leuko-araiosis on magnetic resonance imaging and speed of mental processing. Arch Neurol 1990;47: 151–156.
4. Baddeley AD. Working memory. Science 1992;255:556–559.
5. Rabins RV, Mace NL, Lucas MS. The impact of dementia on the family. JAMA 1982;248:333–335.
6. Pruchco RA, Resch NC. Aberrant behaviors and Alzheimer's disease: Mental health effects on spouse caregivers. J Gerontol 1989;44:S177–S182.
7. Lafosse JM, Reed BR, Mungas D, Sterling SB, Wahbeh H, Jagust WJ. Fluency and memory differences between ischemic vascular dementia and Alzheimer's disease. Neuropsychology 1997;11:514–522.
8. Pierpaoli C, Basser PJ. Toward a quantitative assessment of diffusion anisotropy. Magn Res Med 1996;36:893–906.
9. Chabriat H, Pappata S, Poupon C, et al. Clinical severity in CADASIL related to ultrastructural damage in white matter: in vivo study with diffusion tensor MRI. Stroke 1999;30:2637–2643.
10. Molko N, Pappata S, Mangin JF, et al. Diffusion tensor imaging study of subcortical gray matter in CADASIL. Stroke 2001;32:2049–2054.
11. O'Sullivan, M, Morris RG, Huckstep B, Jones DK, Williams SCR, Markus HS. Diffusion tensor MRI correlates with executive dysfunction in patients with ischaemic leukoaraiosis. J Neurol Neurosurg Psychiatry 2004;75:441–447.
12. Kalaria RN, Ballard C. Overlap between pathology of Alzheimer disease and vascular dementia. Alzheimer Dis 1999;13(suppl 3):S115–S123.
13. Fox NC, Crum WR, Scahill RI, Stevens JM, Janssen JC, Rossor MN. Imaging of onset and progression of Alzheimer's disease with voxel-compression mapping of serial magnetic resonance images. Lancet 2001;358:201–205.
14. Joutel A, Vahedi K, Corpechot C, et al. Strong clustering and stereotyped nature of Notch3 mutations in CADASIL patients. Lancet 1997; 350:1511–1515.
15. Mesulam M-M, Siddique T, Cohen B. Cholinergic denervation in a pure multi-infarct state: observations on CADASIL. Neurology 2003;60: 1183–1185.
16. O'Sullivan, M, Singhal S, Charlton RA, Markus HS. Diffusion tensor imaging of thalamus correlates with cognition in CADASIL without dementia. Neurology 2004;62:702–707.
17. Army Individual Test Battery. The Trail Making Test: Manual of directions and scoring. Washington, DC: War Department, Adjutant General's Office, 1944.
18. Robbins TW. Dissociating executive functions of the prefrontal cortex. Phil Trans Royal Soc Lond Ser B Biol Sci 1996;351:1463–1470.
19. Wechsler D. Wechsler Adult Intelligence Scale–revised. New York: Psychological Corp., 1981.

20. Wechsler D. Wechsler Memory Scale–revised. San Antonio: Psychological Corp., 1987.
21. Jones DK, Horsfield MA, Simmons A. Optimal strategies for measuring diffusion in anisotropic systems by magnetic resonance imaging. Magn Res Med 1999;42:515–525.
22. Smith SM. Fast robust automated brain extraction. Hum Brain Map 2002;17:143–155.
23. Friston KJ, Holmes AP, Worsley KJ, Poline JP, Frith CD, Frackowiak RSJ. Statistical parametric maps in functional imaging: a general linear approach. Hum Brain Map 1995;2:189–210.
24. Poline JP, Worsley KJ, Evans AC, Friston KJ. Combining spatial extent and peak intensity to test for activations in functional imaging. Neuroimage 1997;5:83–96.
25. Talairach J, Tournoux P. Co-planar stereotaxic atlas of the human brain. New York: Thieme, 1988.
26. Morris R, Pandya DN, Petrides M. Fiber system linking the mid-dorsolateral frontal cortex with the retrosplenial/presubicular region in the rhesus monkey. J Comp Neurol 1999;407:183–192.
27. Petrides M, Milner B. Deficits on subject-ordered tasks after frontal- and temporal-lobe lesions in man. Neuropsychologia 1982;20:249–262.
28. Nakahara K, Hayashi T, Konishi S, Miyashita Y. Functional MRI of macaque monkeys performing a cognitive set-shifting task. Science 2002;295:1532–1536.
29. LaBar KS, Gitelman GR, Parrish TB, Mesulam M-M. Neuroanatomic overlap of working memory and spatial attention networks: a functional MRI comparison within subjects. Neuroimage 1999;10:695–704.
30. Courtney SM, Ungerleider LG, Keil K, Haxby JV. Transient and sustained activity in a distributed neural system for human working memory. Nature 1997;386:608–611.
31. Jonides J, Schumacher EH, Smith EE, et al. The role of parietal cortex in verbal working memory. J Neurosci 1998;18:5026–5034.
32. Smith EE, Jonides J, Koeppe RA. Dissociating verbal and spatial working memory using PET. Cereb Cortex 1996;6:11–20.
33. Paulesu E, Frith CD, Frackowiak RSJ. The neural correlates of the verbal component of working memory. Nature 1993;362:342–345.
34. Catani M, Howard RJ, Pajevic S, Jones DK. Virtual in vivo interactive dissection of white matter fasciculi in the human brain. Neuroimage 2002;17:77–94.
35. Behrens TE, Johansen-Berg H, Woolrich MW, et al. Non-invasive mapping of connections between human thalamus and cortex using diffusion imaging. Nat Neurosci 2003;6:750–757.

Neuro*Images*

Figure 1. A photo of a room once belonging to Jean-Martin Charcot. Metropolitan Museum of Art, Mr. and Mrs. Charles Wrightsman Gift (63.228.1), All Rights Reserved.

A room from Jean-Martin Charcot's house at the Metropolitan Museum of Art

Michael H. Pourfar, MD, Manhasset, NY

This room is part of the Decorative Arts Collection at the Metropolitan Museum of Art. The paneling from the room was originally in the house purchased by Charcot but was removed during Charcot's lifetime. A picture of the room at the museum is shown (figure 1), along with a photograph of a room from the same house taken during the period of the Charcot family's residence (figure 2). The pictures are offered to readers of *Neurology* as part of historical iconography and as information on the interface between art and neurology in an American museum collection.

Figure 2. The Charcot room as it appeared during his lifetime. Photograph courtesy of the Vallin-Charcot Archives.

Disclosure: The author reports no conflicts of interest.

Address correspondence and reprint requests to Dr. M.H. Pourfar, North Shore University Medical Center, Department of Neurology, Manhasset, NY 11030; e-mail: Mpourfar@NSHS.edu

A room from Jean-Martin Charcot's house at the Metropolitan Museum of Art

Michael H. Pourfar

Neurology 2005;65;1590
DOI 10.1212/01.wnl.0000182294.09191.26